

# **MEMBER REPORT**

**China**

## **ESCAP/WMO Typhoon Committee The 14th Integrated Workshop**

**Guam, USA**

**November 4–7, 2019**

## CONTENTS

### **I. Overview of Tropical Cyclones Affecting China since Last Annual Meeting of ESCAP/WMO Typhoon Committee**

- 1.1 Meteorological and Hydrological Assessment P.1
- 1.2 Socio-Economic Assessment P.21
- 1.3 Regional Cooperation Assessment P.22

### **II. Progress in Key Research Areas**

- 2.1 Application of Artificial Intelligence Technology in TC Intensity Estimation P.28
- 2.2 Active Participation and Promotion for the Implementation of WIS P.28
- 2.3 Advances in Typhoon Numerical Model P.29
- 2.4 Assessment of Subjective Forecasts and Numerical Model Forecasts P.31
- 2.5 Advances in TC Real-Time Observations P.33
- 2.6 Advances in Scientific Researches on Tropical Cyclones P.35
- 2.7 Improving Typhoon Forecasting and Warning Services, and Disaster Emergency Rescue P.38
- 2.8 CMA Trainings of Operational Skills on Tropical Cyclones P.41
- Annexes P.45

## **I. Overview of Tropical Cyclones Affecting China since Last Annual Meeting of ESCAP/WMO Typhoon Committee**

### **1.1 Meteorological and Hydrological Assessment**

A distinct central Pacific (CP) El Niño event maintained over the tropical central and eastern Pacific from January to June, 2019. Since May, the warm state over the tropical eastern Pacific has been weakening, resulting in the end of El Niño event in July. However, the warm state over the tropical central Pacific continued. In general, the CP El Niño event could lead to a farther north path of tropical cyclones (TCs) affecting China. Besides, the lasting warmer water in the tropical northern Indian Ocean during the spring and the summer of 2019 leads to less TC genesis over the northwestern Pacific.

From January 1 to October 17, 2019, the northwestern Pacific and the South China Sea witnessed the generation of 19 TCs, including tropical storms, severe tropical storms, typhoons, severe typhoons and super typhoons. Of them, 5 TCs made landfall over the coastal areas of China, namely, tropical storm Mun (1904), tropical storm Wipha (1907), super typhoon Lekima (1909), severe tropical storm Bailu (1911) and typhoon Mitag (1918). It is 1.7 less than the multi-year average number (6.7).



## **2) Lower TC Intensity**

The average peak intensity of the 19 TCs in 2019 is 35.9 m/s, which is significantly lower than the multi-year average (38.2 m/s).

## **3) Fewer Landing TCs**

5 of the 19 TCs made landfall over the eastern and southern coastal areas of China, which is 1.7 less than the multi-year average (6.7) in the same period.

## **4) Generally Low-Intensity Landing TCs with Extremely High-Intensity Case**

The average landing intensity of the 5 TCs is 30.6 m/s, lower than the multi-year average (32.6 m/s). In fact, the landing TCs in 2019 are generally weak, except an extremely strong one. For example, Lekima, landing at 0145 LST on August 10 over the coastal area of Wenling City, Zhejiang Province, has the maximum winds up to of 52 m/s and the minimum central pressure of 930 hPa.

## **5) Farther Northward and Westward Origins of TC**

The average genesis location of 19 typhoons in 2019 is 17.7° N, 133.1° E, which is farther northward and westward than the historical average location (16.1° N, 136.5° E).

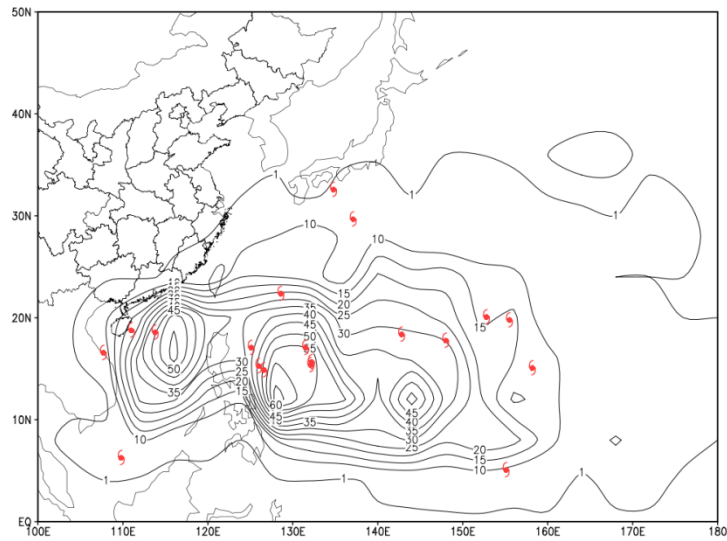


Fig. 1.4 Density distribution (contour; resolution:  $2.5^{\circ} \times 2.5^{\circ}$ ) of TC genesis locations in the northwestern Pacific and the South China Sea during 1949 – 2018, and the genesis locations of TCs from January 1 to October 17, 2019

### 1.1.2 Precipitation Characteristics of TCs Affecting China

Since the beginning of 2019, 19 TCs have generated over the northwestern Pacific and the South China Sea, 5 of which made landfall over China. Among them, 2 TCs landed at the area from the western Guangdong Province to the eastern Hainan Province, 1 TC landed at Fujian Province and 2 TCs landed at Zhejiang Province. In particular, typhoon Lekima (1909) brought a great impact on China's rainfall-flood regime. It mainly shows the following two features.

#### 1) Wide-Range Rainfall and High-Intensity Rainstorms

According to the monitoring results from hydrological department (the same below), TCs have affected 18 provinces, namely, Hainan, Guangdong, Guangxi, Yunnan, Fujian, Taiwan, Zhejiang, Jiangsu, Anhui,

Hubei, Jiangxi, Henan, Shandong, Hebei, Liaoning, Jilin, Heilongjiang, and Shanghai. In particular, typhoon Lekima (1909) successively affected 13 provinces (municipalities) in 6 river basins (Yangtze River Basin, Taihu Lake Basin, Huaihe River Basin, Yellow River Basin, Haihe River Basin and Songliao River Basin). The impact lasted up to 8 days (August 9–16). It is the third strongest typhoon landing on Zhejiang since 1949, ranking the fifth based on the typhoon landing intensity over the mainland of China. The area with the total rainfall more than 400 mm is 7000 km<sup>2</sup>, and that with rainfall over 250 mm is 51000 km<sup>2</sup>. The maximum accumulated rainfall is 927 mm (from 0800 LST on August 8 to 1600 LST on August 10) at the Fuxi reservoir of Wenzhou, Zhejiang, breaking the historical record of Zhejiang (the maximum accumulated rainfall caused by the severe typhoon Rananim in 2004 is 905 mm in Feitou Village, Yueqing City).

## **2) Many rivers exceeding the flood warning level, some breaking historical records**

In total, typhoon precipitation has caused floods exceeding the warning level in 206 rivers of 12 provinces, including Hainan, Guangdong, Guangxi, Zhejiang, Jiangsu, Shanghai, Anhui, Jiangxi, Shandong, Liaoning, Jilin and Heilongjiang. Among them, 10 rivers, namely, Shifeng River in Zhejiang, Wusong River (a tributary of Huangpu River) in Shanghai, Shuiyang River in Anhui, Xinyi River in

Jiangsu, Mi River, Sha River, Xiaoqing River and its tributary Xiaofu River in Shandong, Shuangyang River and Wangqing River in Jilin, claimed the historical record of flood, and the Linhai tide station in Zhejiang Province reported the high tide level breaking the historical record.

### **1.1.3 TCs Affecting China**

#### **1) Tropical Storm Mun (1904)**

Tropical storm MUN formed over the eastern coastal waters of Hainan Island at 1300 UTC on 2 July 2019. MUN made landfall over Wanning, Hainan Province at 1645 UTC on July 2 with the maximum wind speed 18 m/s and minimum sea level pressure 992 hPa.

After landfall, Mun continued to move westward, entering the Beibu Gulf around 0400 UTC on July 3, and landed for the second time over the coastal area of Taiping Province in Vietnam at 2245 UTC on July 3 with the maximum wind speed of 18 m/s and the minimum sea level pressure 992 hPa. At 0000 UTC on July, 4, Mun weakened into a tropical depression, and it stopped being registered at 0900 UTC in Vietnam.

Under the impact of Mun, the accumulated rainfall over the central and southern Hainan Island, the central coastal area of Guangdong, the southern Fujian and Fangchenggang of Guangxi reached 100–170 mm from July 2 to July 4. The maximum rainfall in Changjiang County of Hainan Island is 262 mm, and the maximum hourly precipitation in the

above-mentioned areas is 40–89 mm. During this period, there were gales up to 6–8 scales over most parts of Hainan Island, west-central and coastal areas of Guangdong and southern coastal areas of Guangxi, with some gusts reaching scale 9–10.

The impact of Mun has more benefit than disadvantages. The rainfall brought by it has effectively alleviated the drought in Hainan Island, southern Guangxi and Leizhou Peninsula in Guangdong, and has cooled the high temperature weather in South China. According to the report from Hainan Provincial Emergency Management Department, the reservoir water storage in Hainan Province has increased by about 98 million tons.

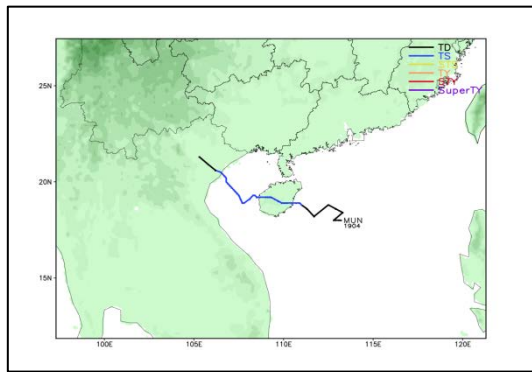


Fig. 1.5a The track of Mun

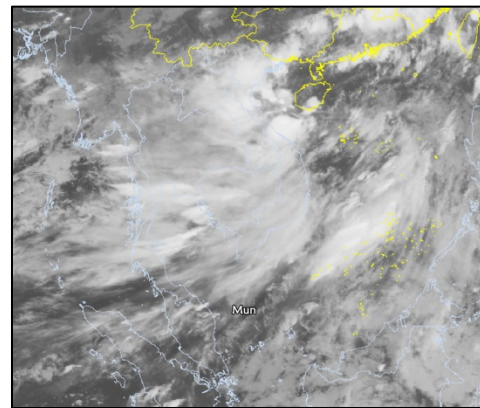


Fig. 1.5b FY-4A Satellite image of Mun

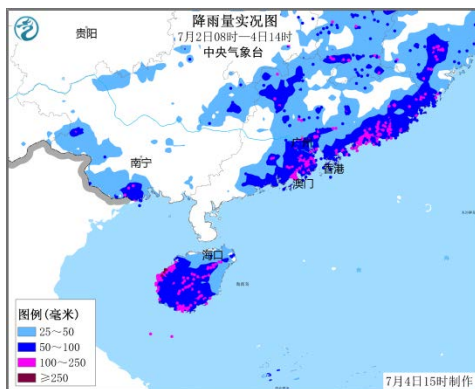


Fig. 1.5 c MUN’s accumulated rainfall (0000 UTC July 1 to 0000 UTC July 5)



Fig. 1.5 d hazards brought by Mun

## **2) Tropical Storm Wipha (1907)**

Tropical storm WIPHA (1907) formed over the northwestern part of South China Sea at 0000 UTC on July 31. It continued to move northwestward and made its landfall over Wenchang, Hainan Province at 1750 UTC of July 31, with the maximum wind speed reaching 23 m/s and the minimum sea level pressure of 985 hPa.

After whirling around the northeastern Hainan Island, Wipha turned northward and made its second landfall over Zhanjaing, Guangdong Province at 0940 UTC of August 1, with the maximum winds 23 m/s and the minimum sea level pressure 985 hPa. Then Wipha turned westward, entered the northern Beibu Gulf and landed over Fangchengang, Guangxi Zhuang Autonomous Region at 1320 UTC of August 2, with the maximum wind speed of 23 m/s and the minimum sea level pressure 985 hPa. Finally, Wipha moved southwestward, entered Vietnam and weakened into a tropical depression at 0600 UTC on August 3. Afterwards, it continued to weaken and stopped being registered at 1500 UTC of August 3.

Under the impact of Wipha, the accumulated rainfall over the western and northern Hainan Island, southwestern and coastal areas of Guangdong and southeastern coastal areas of Guangxi reached 200–300 mm. In Dongfang of Hainan Island, Jiangmen, Yangjiang and Maoming of Guangdong, Fangchenggang and Qinzhou of Guangxi, the

accumulated rainfall reached 400–484 mm. The maximum hourly rainfall is within 60–112 mm. During this period, there were gales up to 7–9 scales over the north-central Hainan Island, the south-central Guangdong and southern coastal areas of Guangxi, with some gusts reaching scale 10–11.

Due to the joint influence of the rainfall brought by Wipha and the astronomical tide, 27 small and medium rivers (Xinwu River—a tributary of Nandu River in Hainan, Luoding River and Lezhu River—tributaries of Xijiang River in Guangdong, Aojiang River in the east coast of Guangdong, Yongning River section of Yujiang River and Mingjiang River—a tributary of Yujiang River in Guangxi, Danzhu River and Beilun River in the south coast of Guangxi, etc.) reported floods that exceeded the warning level. The maximum exceeding range is within 0.03–3.15 m. 22 tide stations in Hainan and Guangdong reported high tide levels exceeding the warning level by 0.01–0.89 m.

By the end of August 4, Wipha has affected 334,000 people from 46 counties (cities and districts) of 15 cities in Guangdong, Guangxi and Hainan; 21,000 people have been relocated; more than 70 houses collapsed, and over 270 houses have been damaged at different degrees; 72,300 hectares of crops have been affected, 1,300 hectares of which failed; and its direct economic losses has amounted to 170 million yuan.

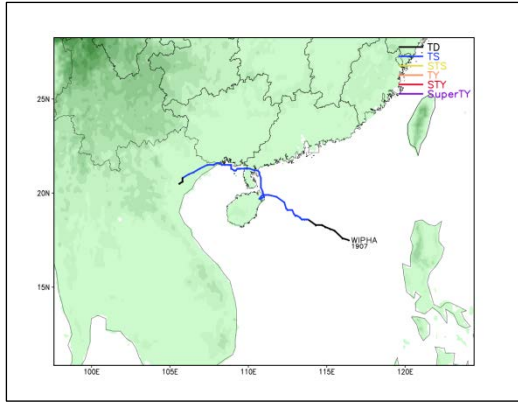


Fig. 1.6a The Track of Wipha

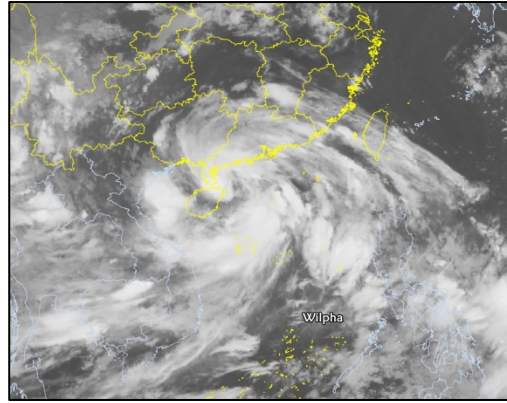


Fig. 1.6b FY-4A Satellite image of Wipha

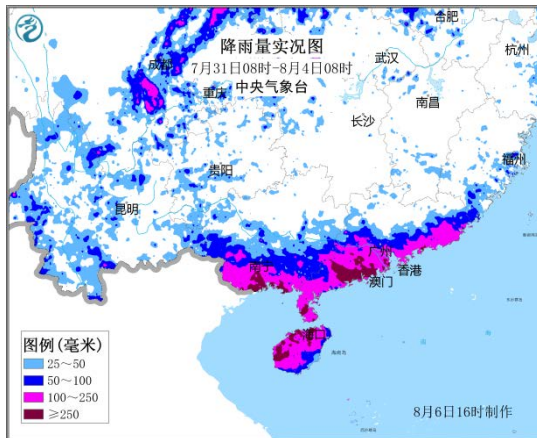


Fig. 1.6c Wipha's accumulated rainfall (0000 UTC July 31–0000 UTC August 4)



Fig. 1.6d hazards brought by Wipha

### 3) Super Typhoon Lekima ( 1909)

At 0900 UTC on August 4, tropical storm Lekima (1909) formed over the ocean east of the Philippines, and then moved northwestward. It intensified into a severe tropical storm at 1800 UTC on August 5, and became a typhoon at 2100 UTC on August 6. It strengthened to a severe typhoon at 0900 UTC on August 7, and then a super typhoon at 1500 UTC on August 7. Within 24 hours, it rapidly intensified from a severe tropical storm to a super typhoon. Lekima made landfall over Wenling, Zhejiang Province at 1745 UTC on August 9, with the maximum wind speed 52 m/s and the minimum sea level pressure 930 hPa. After the

landfall, Lekima began to weaken, and moved northward. It weakened into a tropical storm in the northern Zhejiang at 1200 UTC on August 10. After moving northward and crossing the eastern Jiangsu, it entered the Yellow Sea at 0400 UTC on August 11. Then, Lekima made its second landfall over Qingdao, Shandong at 1250 UTC on August 11, with the maximum wind speed 23 m/s and the minimum sea level pressure 980 hPa. After crossing Shandong Peninsula, Lekima entered Laizhou Bay at 2100 UTC on August 11, and weakened into a tropical depression at 0000 UTC on August 13 after whirling. Lekima disappeared at 0600 UTC on August 13.

Lekima is the strongest typhoon making landfall over China this year, ranking the fifth among the typhoons landing on the mainland of China since 1949, and the third among the typhoons landing on Zhejiang. After landfall, Lekima moved slowly and lingered over land for 44 h, including 20 h in Zhejiang Province.

Affected by Lekima, extreme heavy rainfall occurred in Zhejiang, Shandong, Jiangsu and other areas, with the average rainfall of 165 mm in Zhejiang. The total rainfall in Kuocangshan of Linhai reached 833 mm, ranking the second in Zhejiang caused by landing typhoons (the first is 916 mm in Feitou, Yueqing, caused by Rananim in 2004). The average rainfall in Shandong is 158 mm, exceeding that caused by typhoon Rumbia in 2018 (135.5 mm) and becoming the maximum rainfall event in

Shandong on record. During this period, the daily rainfall of 35 meteorological observation stations in Zhejiang, Shandong and other areas broke the local historical record of August, among which 24 stations broke the local historical record, with the most stations of breaking records in Shandong.

Gales up to scale 8 occurred over coastal areas of Fujian, Zhejiang, Shanghai, Jiangsu, Anhui, Shandong, Hebei, Tianjin, Liaoning and other regions. Among them, the coastal winds in Zhejiang generally reached scale 12–14, and scale 15–17 in some islands. The coastal wind over scale 10 lasted for nearly 36 h, and the winds over scale 12 lasted for about 20 h. The maximum gust is up to 61.4 m/s in Sansuan Island, Shitang Town, Wenling City. The observed wind speed of Lekima ranks the second among the typhoons landing over Zhejiang Province.

Due to the heavy rainfall caused by Lekima, floods exceeding warning level occurred in 139 rivers in 8 provinces or municipalities, including Zhejiang, Jiangsu, Shanghai, Anhui, Shandong, Liaoning, Jilin and Heilongjiang. The maximum exceeding range is within 0.01–4.48 m. 54 rivers reported floods exceeding the guarantee line. 10 rivers (Shifengxi River in Zhejiang, Wusong River—a tributary of Huangpu River in Shanghai, Shuiyang River in Anhui, Xinyi River in Jiangsu, Mi River, Sha River, Xiaoqing River and its tributary Xiaofu River in Shandong, Shuangyang River and Wangqing River in Jilin, etc.) claimed

the historical record of flood. Among them, the No.1 flood of 2019 occurred in Songhua River, Yi River and Shu River in Shandong. Especially, the flood in Mi River in Shandong was of the return period of 50 years. Besides, 7 coastal tide stations in Zhejiang, Shanghai and Jiangsu had tides exceeding warning level, and 1 tide station reported high tide levels that exceeded historical record.

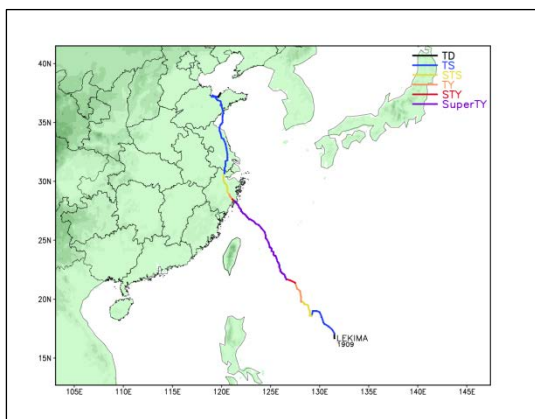


Fig. 1.7a The Track of Lekima

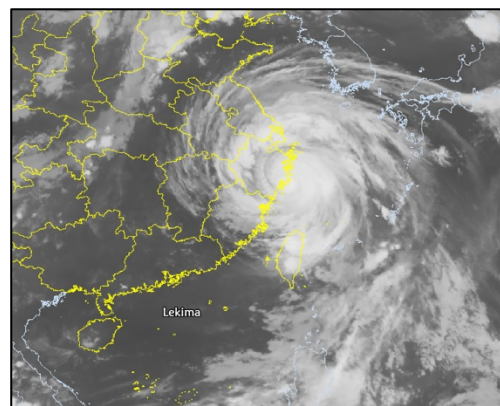


Fig. 1.7b FY-4A Satellite image of Lekima

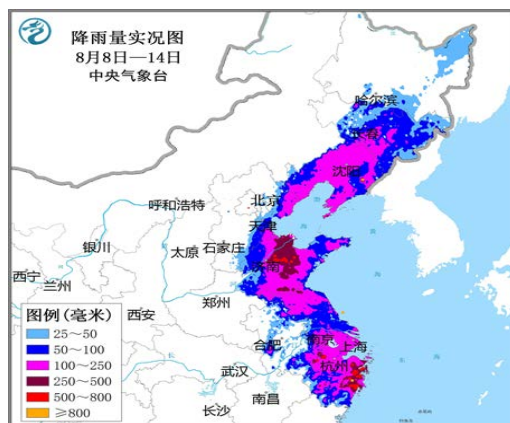


Fig. 1.7c Lekima's accumulated rainfall (0000 UTC August 8–0000 UTC August 14)



Fig. 1.7d hazards brought by Lekima

#### 4) Severe Tropical Storm Bailu (2011)

At 0600 UTC on August 21, tropical storm Bailu (2011) formed over the northwestern Pacific, and moved northwestward then intensified.

It became a severe tropical storm at 1500 UTC on August 22, and made landfall over the coastal area of Pingtung County, Taiwan Province at 0500 UTC on August 24, with the maximum wind speed 30 m/s and the minimum sea level pressure 980hPa. Then Bailu continued to move northwestward and entered the Taiwan Strait. At 2325 UTC on August 24, it made the second landfall over the coastal area of Zhangzhou, Fujian, with the maximum winds 25 m/s and the minimum sea level pressure 988 hPa. After the landfall, it gradually weakened, and stopped being registered over northern Guangdong at 2100 UTC on August 25.

Under the influence of Bailu, the accumulated rainfall in the eastern and southern Taiwan reached 200–600 mm, and that in Taidong exceeded 700 mm. In coastal areas of Zhejiang, southern Fujian, east-central Guangdong, southern Jiangxi, southern Hunan and southeastern Guangxi, the accumulated rainfall was within 50–150 mm, while Guangzhou, Zhuhai, Zhaoqing, Jieyang, Huizhou and Heyuan in Guangdong as well as Yulin, Guigang, Wuzhou and Hezhou in Guangxi had rainfall of 200–284 mm.

Gales of scale 8–10 occurred in Taiwan Province, and gusts of scale 11–14 were observed in Taidong County and Nantou County. Gales of scale 8–10 occurred in coastal areas of Zhejiang, southern Fujian and its coastal areas, central and southeastern coastal areas of Guangdong, southern Jiangxi, southern Hunan and other areas. Gusts of scale 11–13

occurred in coastal areas of Fujian.

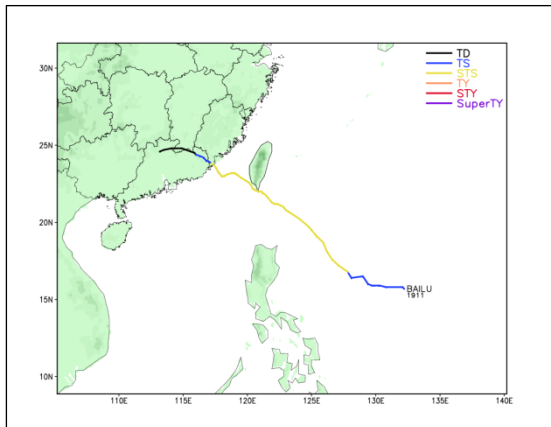


Fig. 1.8a The Track of Bailu

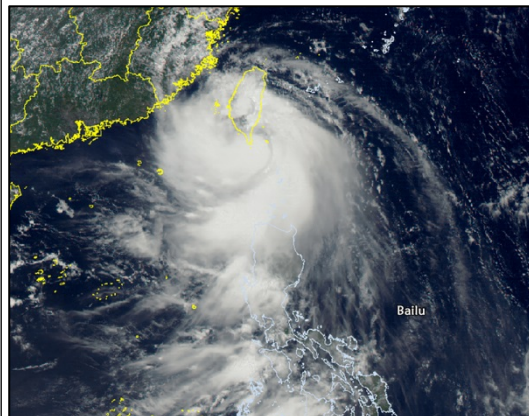


Fig. 1.8b FY-4A Satellite image of Bailu

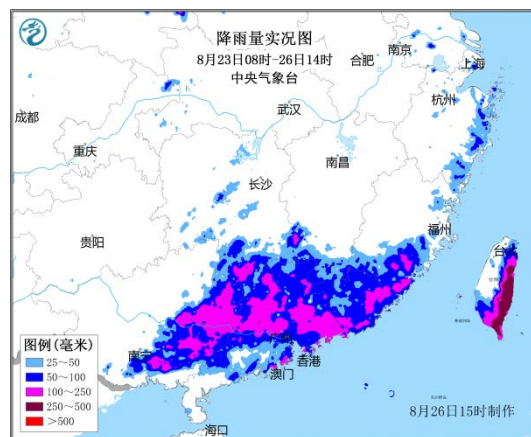


Fig. 1.8. Bailu's accumulated rainfall (0000 UTC August 23–0600 UTC August 26)

## 5) Super Typhoon Lingling (1913)

Tropical storm LINGLING (1913) was named at 0000 UTC on September 2. After genesis, Lingling moved northwestward and became a strong tropical storm. At 1200 UTC on September 3, it turned to be a typhoon, and strengthened to be a severe typhoon at 2100 UTC on September 4, then intensified to be a super typhoon at 0200 UTC on September 5. Subsequently, it moved northward and crossed the East China Sea and the Yellow Sea. Around 0550 UTC on September 7, it

landed on the southwest coastal area of Hwanghaenam-do in North Korea. During the landfall, the maximum wind speed reached 38 m/s, and the minimum sea level pressure 960 hPa. After landfall, Lingling continued to move northward, and entered Jilin Province and Heilongjiang Province respectively around 1300 UTC and 1800 UTC on September 7. It finally stopped being registered in Russia at 0300 UTC on September 8.

Under the impact of Lingling, the rainstorm and downpour occurred in the east-central Northeast China from June 6 to June 8. The rainfall in Lanxi of Heilongjiang Province is 233 mm; the daily rainfall at 26 stations in Heilongjiang, Jilin and Liaoning broke the historical record in September since the station was built. Gusts of scale 7–9 occurred in the Shandong Peninsula, the northern Liaoning and Liaodong Peninsula, the east-central Jilin and the east-central Heilongjiang, while gusts of scale 10–13 occurred locally in the northeastern Jilin and the southeastern Heilongjiang.

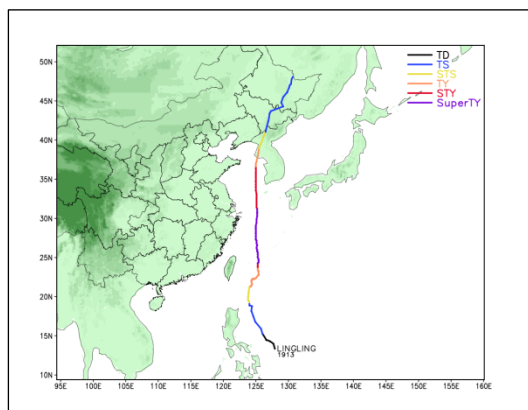


Fig. 1.9a The Track of Lingling

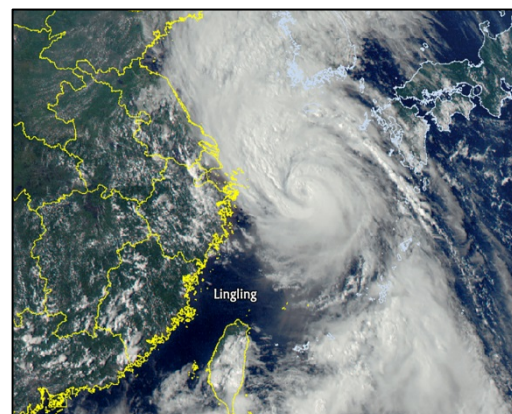


Fig. 1.9b FY-4A Satellite image of Lingling

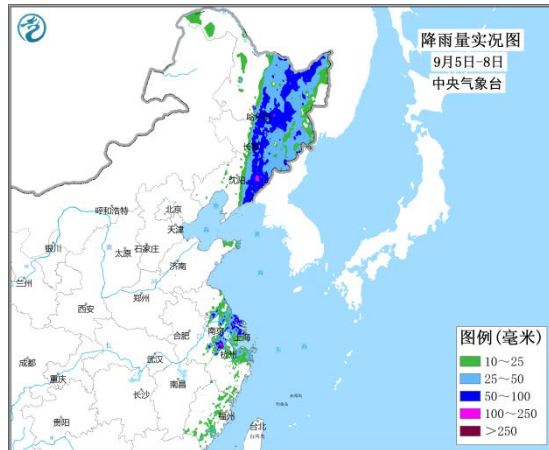


Fig. 1.9c Lingling's accumulated rainfall (0000 UTC September 5–0000 UTC September 8)

## 6) Typhoon Mitag (1918)

At 0000 UTC on September 28, typhoon Mitag (1918) formed over the ocean east of the Philippines, then moved northwestward with an increasing intensity. At 2100 UTC on September 28, it became a strong tropical storm, and intensified into a typhoon at 0900 UTC on September 29. On September 30, it began to move northward, and made landfall over the coastal area of Zhoushan City, Zhejiang at 1230 UTC on October 1, with the maximum wind speed 30 m/s and the minimum sea level pressure 980 hPa. Mitag then moved northeastward, and its intensity began to decrease gradually. At 1210 UTC on October 2, it made landfall again on the coastal area of Jeollanam-do, South Korea, with the maximum wind speed of 23 m/s and the minimum sea level pressure of 988 hPa. After crossing the southern Korean Peninsula, it entered the Sea of Japan, and then weakened and disappeared.

Under the impact of Mitag, from September 30 to October 1, the

accumulated rainfall in the eastern Zhejiang, the eastern Shanghai and some parts of the north-central Taiwan Island exceeded 100 mm; the rainfall in Ningbo, Zhejiang was within 250–335 mm; and the rainfall in Zhoushan reached 268–444 mm. Eastern Zhejiang and Taiwan Island recorded gusts of scale 12–14 in some places, and the gust in Pingyu, Pingyang County, Wenzhou reached scale 16 (52.2 m/s).

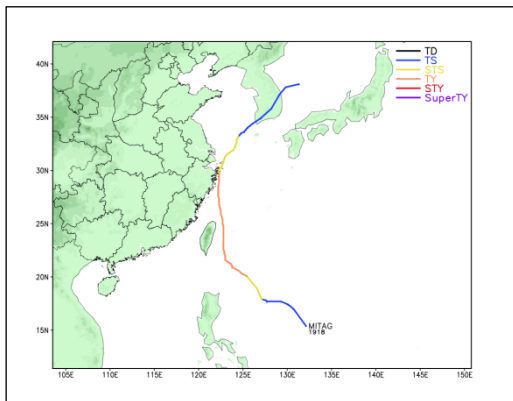


Fig. 1.10a The track of Mitag

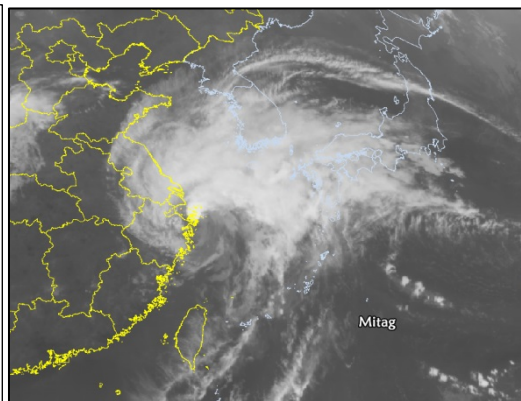


Fig. 1.10b FY-4A satellite image of Mitag



Fig. 1.10c Mitag's accumulated rainfall (0000 UTC September 30–0000 UTC October 2)



Fig. 1.10d hazards brought by Mitag

### 1.1.5 Climatic Prediction of TCs

In each March and May, the National Climate Center (NCC) conducts seasonal predictions on the number of TC generation, the landing-TC number, the possible moving path and intensity of TCs in the northwestern Pacific and the South China Sea. The predictions are made

by both the physical statistics and the dynamic models. Recently, an objective interpretation and application method based on the output of high-resolution climate model has been used in the operation. Verification results indicate that the method is skillful in predicting the number of TC generation (Figs. 1.11a and 1.11b), the path density (Fig. 1.11c) and the accumulated cyclone energy (ACE, Fig. 1.11d). Based on the above methods, the comparison between the seasonal prediction issued by NCC and the observation is shown as follows.

### **1) TC Prediction for the whole of 2019**

It was predicted that there would be 23–25 TCs in 2019, less than the multi-year average (26). Among them, 7–8 TCs would land on China, which is close to or slightly more than the multi-year average. The general intensity of the landing TCs would be higher, with most of them moving westward.

### **2) TC Prediction for the summer of 2019**

In May of 2019, NCC predicted that the number of TCs in the following summer would be within 8–10, less than the multi-year average (11). Among them, 4–5 TCs would land on China, which is close to the multi-year average (4.6). In observation, 10 TCs generated, less than the multi-year average. Among them, 4 landed on China, totally in accordance with the prediction. Besides, it was predicted that the first landfall would be late than normal, which is completely consistent with

the observation as well.

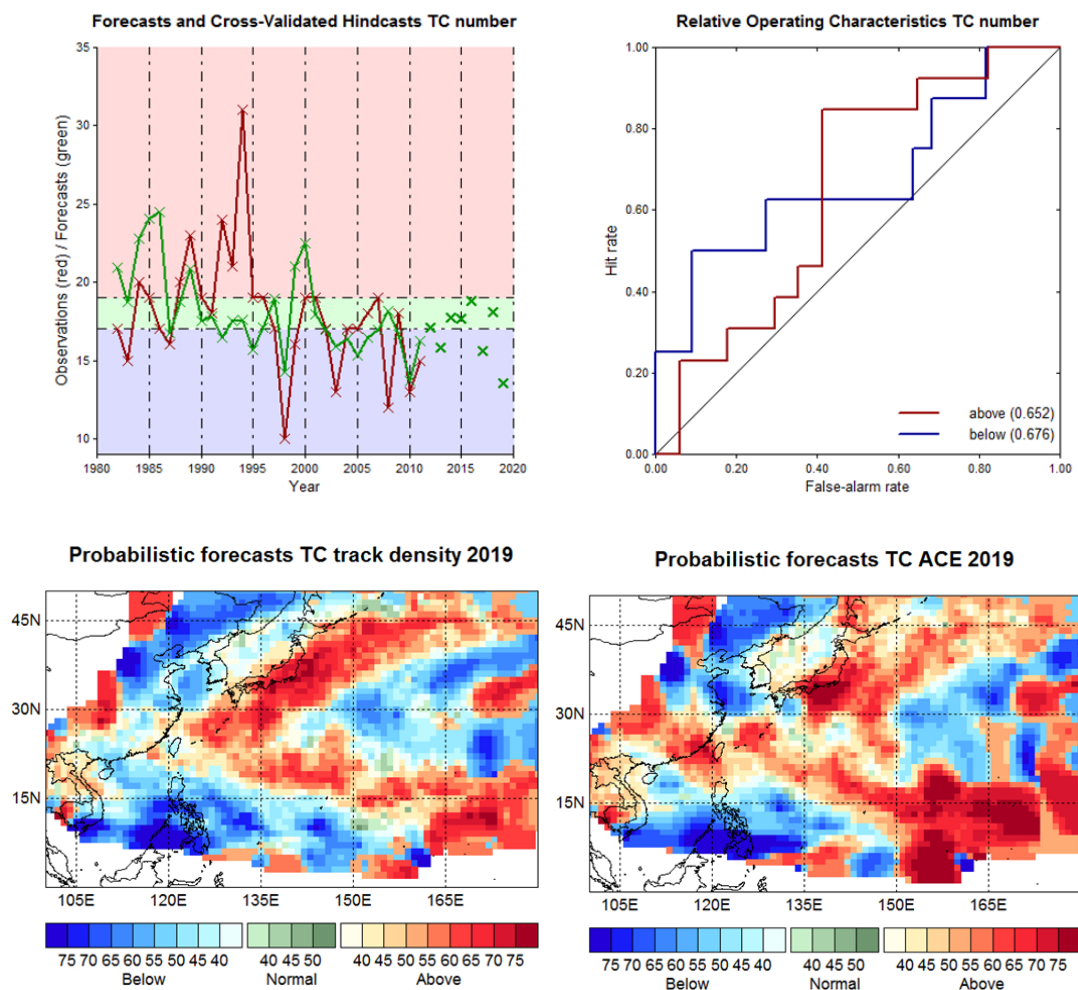


Fig. 1.11 Predictions of TC activities during July–October of 2019 based on the Canonical Correlation Analysis method of the ensemble-predicted geopotential height field from the NCEP CFS v2 model with an initial time of late March: (a) probability prediction of the TC number for a 3-category classification (fewer, normal and more); (b) cross-hindcast ROC verification; (c) moving-path density prediction of TCs over the northwestern Pacific; and (d) ACE prediction of TCs over the northwestern Pacific

## 1.2 Socio-Economic Assessment

Since the beginning of 2019, 5 TCs have made landfall over and affected China, striking 16.491 million people from 16 provinces (autonomous regions and municipalities). The number of dead or missing people reached 76, and 2.462 million people have been evacuated and resettled. 16,000 houses collapsed, and 136,000 were damaged. 1,781,700

hectares of crops have been affected, 156,800 hectares of which failed.

Typhoon Lekima caused the heaviest losses, with the highest landfall intensity in 2019. A total of 14.024 million people were affected in 353 counties (cities and districts) and 59 cities (municipalities) of 10 provinces (municipalities), including Hebei, Liaoning, Jilin, Shanghai, Jiangsu, Zhejiang, Anhui, Fujian, Shandong and Taiwan. 71 people were killed or missing as a result of the disaster; 2.097 million people were evacuated and resettled; and 51.53 billion yuan of direct economic losses were incurred.

Table 1.1 Impacts of TCs landing over China in 2019

<b>Typhoon name and number</b>	<b>Landing locations</b>	<b>Landing date and intensity</b>	<b>Affected provinces</b>	<b>Affected population (10<sup>4</sup> people)</b>	<b>Death toll (Person)</b>	<b>Emergently evacuated population (10<sup>4</sup> people)</b>
Wipha (1907)	Wenchang, Hainan	Aug. 1 (tropical storm)	Guangdong, Guangxi, Hainan	43.3	0	2.7
Lekima (1909)	Wenling, Zhejiang	Aug. 10 (super typhoon)	Hebei, Liaoning, Jilin, Shanghai, Jiangsu, Zhejiang, Anhui, Fujian, Shandong, Taiwan	1402.4	71	209.7
	Qingdao, Shandong	Aug. 11 (tropical storm)				
Bailu (1911)	Zhangzhou, Fujian	Aug. 25 (severe tropical storm)	Fujian, Jiangxi, Hunan, Guangdong, Guangxi, Taiwan	22.0	1	6.1
Lingling (1913)			Zhejiang, Jilin, Heilongjiang	99.4	0	0.4
Mitag (1918)	Zhoushan, Zhejiang	Oct. 1 (severe tropical storm)	Shanghai, Zhejiang	82.0	4	27.3
<b>Total</b>				<b>1649.1</b>	<b>76</b>	<b>246.2</b>

Note: Affected by Bailu and Lekima, 2 people died in Taiwan, and the data is from the Internet

## **1.3 Regional Cooperation Assessment**

### **1.3.1 12th China-Korea Joint Workshop on TCs**

The 12th China-Korea Joint Workshop on TCs was held in China on May 20–24, 2019. The workshop was co-organized by China Meteorological Administration (CMA) and Korea Meteorological Administration (KMA), and was hosted by Shanghai Meteorological Service and Shanghai Typhoon Institute (STI).

Focusing on the topics of TC intensity and dynamics research, structural analysis and observation research, prediction technology, climate, engineering and storm warning, nearly 30 experts and scholars from meteorological communities of China and South Korea, Fudan University, Nanjing University, Beijing Normal University, National University of Defense Technology, Nanjing University of Information Science and Technology and other universities exchanged and discussed the latest progress in researches and prediction of TCs, effectively promoting the bilateral exchange between China and South Korea in TCs.



Fig. 1.12 The 12th China-Korea Joint Workshop on TCs was held in Shanghai

During the workshop, the KMA delegation also visited Beijing and had operational exchange and discussion with experts of typhoon and marine weather forecasts in NMC, CMA on May 23. The director of National Typhoon Center of Korea, Mr. JUNG Jong Woon introduced the current operations, main skills for typhoon forecasting and operational development. Ms. Xiang Chunyi, forecaster from CMA introduced the progress of CMA's typhoon and marine weather forecast operation, as well as the application of various kinds of observations, numerical model forecasts and subjective comprehensive forecasts. This meeting aims to promote the scientific research and technical cooperation on TC monitoring and forecasting services, together contributing to the progress of TC forecasting operations in the northwestern Pacific.



Fig. 1.13 TC operational exchange and discussion between CMA and KMA in Beijing

### **1.3.2 Joint Conference with Vietnam on TCs**

To effectively make the active cooperation between China and the countries along the Belt and Road in the meteorological forecast and early warning, promote the co-prevention and co-management mechanism in dealing with typhoons and related disasters and earnestly fulfill our international obligations, China and Vietnam have launched real time discussion on typhoons many times in recent years, laying a good foundation for the effective cooperation. For example, for super typhoon Mangkhut in 2018 and tropical storm Mun in 2019, China and Vietnam have held the telephone conference to discuss their future track, intensity and possible precipitation impact on the northern Vietnam.

On 31 July 2019, a half-hour telephone conference was held between the forecasters from NMC of CMA and the experts from the National Hydro-Meteorological Service of Vietnam (NHMS) on typhoon

Wipha which just generated then. The two sides discussed the forecast path, the possible maximum intensity, the time of entering the Beibu Gulf and the landing intensity in the later period of Wipha. During the conference, the two sides effectively communicated the basis for determining the typhoon intensity over the South China Sea, and clarified the need for timely communication about the latest forecast opinions and sharing the observation data in the later stage. Finally, the Chinese side pointed out that the slow moving of Wipha in the later period might bring long lasting precipitation to South China and North Vietnam, which needed close attention.

Since then, with the help of typhoon International Conference platform (web version), China and Vietnam have conducted many real-time online discussions on the real-time positioning and intensity estimation of Wipha. It not only greatly improves the convenience and timeliness of communication between the two sides, but also help more intuitively explain the reasons for prediction and analysis with various observation data and products, which will further improve and promote the extensive application of the platform in the future.



Fig. 1.14 CMA forecasters discussed Wipha’s forecasting with Viet Nam’s colleagues through web-based discussion platform



Fig. 1.15 Web-based discussion platform

### 1.3.3 The Progress of the Journal *Tropical Cyclone Research and Review*

The third issue of 2019 *Tropical Cyclones Research and Review* (TCRR) has been published. The third and fourth issues of 2019 are special issues on the WMO International Workshop on Tropical Cyclones. In addition, Prof. Kimberly Wood from the Mississippi State University

participated the Typhoon Committee fellowship for visiting editor from March 24 to 29, 2019. Prof. Shishir Dube from Indian Institute of Technology visited the TCRR editorial office from October 13 to 19, 2019. The 3rd Editorial Committee Meeting will be held jointly with IWS in Guam.

## **II. Progress in Key Research Areas**

### **2.1 Application of Artificial Intelligence Technology in TC Intensity Estimation**

Based on the historical TC satellite images and TC best track dataset, an intelligent TC intensity estimation technology has been preliminarily developed. This technology has expanded and trained the basic dataset by using deep learning and multimodal convolutional neural network, thus the typhoon intensity can be estimated according to the characteristics of the cloud images. The results showed that the average absolute error of its estimation is within 3 m/s (Fig. 2.1), which is valuable for operational applications.

**Contact Information:** National Meteorological Centre of CMA

### **2.2 Active Participation and Promotion for the Implementation of WIS**

In 2019, Beijing GISC and four product centers (Data Collection and Production Center) of CMA have been running stably, providing FY satellite products, global mesoscale numerical weather prediction products from GRAPES, ensemble forecast products, typhoon model ensemble forecast products, Global/Asian climate monitoring products and other data access services for members of responsible regions such as North Korea, Mongolia, Nepal, Pakistan, Hong Kong, China, Macao,

China and other WMO members in the Asia Pacific region. 1,705 pieces of metadata have been released to 156 registered users, and about 740 GB service data have been provided every day. Beside, since September 2015, in response to the needs of WIS implementation and data access, CMA has provided CMACast, MICAPS and WIS-related technical trainings to Pakistan, North Korea, Myanmar, Laos, Mongolia and other Asian WMO members. CMA has played a positive role in promoting the implementation of WIS in Asia (Fig. 2.2).

**Contact Information:** National Meteorological Information Center of CMA.

### **2.3 Advances in Typhoon Numerical Model**

(1) In 2019, the South China Sea typhoon model TRAMS has been further upgraded in four aspects: model resolution, computational efficiency, dynamical core and physical processes. First, the model resolution has been updated from 18 km to 9 km, and the model covers the area of 70°E–160°E, and 0.8°N–54.8°N. The new model can provide 72–168 h forecasts at an interval of 6 h. As I/O processes and initialization processes are optimized, the parallel efficiency of TRAMS is effectively improved. Meanwhile, the cumulus parameterization scheme and the surface scheme are improved to fit the higher model resolution. In addition, the upgraded 3-D reference atmosphere scheme increases the computational accuracy and stability of the model. By

comparing the new and old versions with the same samples in 2017, it is found that the new version systematically improves the 0–72 h intensity forecast, reducing the mean forecast error by about 1.5 hPa at each forecast time (Fig. 2.3). The TC path forecast in the new version is also better than the old one, and the 72 h forecast error of path is decreased by 13.6 km. In summary, TRAMS-v3.0 has a better performance than TRAMS-v2.0.

(2) The Typhoon Regional Assimilation and Prediction System (T-RAPS) has been applied in the routine operational work. T-RAPS is a set of quasi-operational typhoon prediction system for the northwestern Pacific (including the South China Sea) (Fig. 2.4). It can produce the real-time prediction according to the typhoon real-time location and intensity estimation.

Based on the WRF-ARW model framework, the T-RAPS is coupled with the ROMS ocean model. Besides, it integrates the dynamic initialization of the open ocean typhoon vortex, the semi ideal typhoon vortex initialization with the mesoscale terrain adaptation, the spectral approximation, the cyclic warm start, the CAMS cloud microphysical parameterization scheme, the E- $\epsilon$  boundary layer parameterization scheme, the New Tiedtke cumulus convection parameterization scheme etc. T-RAPS also has a standardized post-processing module with 32 types of products in 5 categories, a product release web page and an

inspection module. The real-time prediction products of T-RAPS have been applied in the daily national weather consultation, the national typhoon emergency response services and other typhoon public prediction services.

**Contact Information:** Guangzhou Institute of Tropical and Marine Meteorology  
Chinese Academy of Meteorological Sciences

## **2.4 Assessment of Subjective Forecasts and Numerical Model**

### **Forecasts**

The TC path and intensity of subjective forecasts and deterministic numerical forecasts are assessed.

#### **(1) Assessment of TC Track Forecasts**

In 2018, the official TC track forecast errors for 24 h, 48 h, 72 h, 96 h and 120 h are 63.2–90.6 km, 109.1–138.1 km, 179.4–196.7 km, 272.9–305.5 km and 418.8–453.8 km, respectively. Through the comparison of 24 h, 48 h and 72 h track forecast errors of several official typhoon prediction agencies in recent years, it can be found that the performance of official subjective track predictions for 24 h and 48 h have been improved steadily, and the performance of 72 h track prediction has improved when compared with those in 2016 and 2017, while closes to that in 2015 (Fig. 2.5).

The error ranges of TC track prediction for 24 h, 48 h, 72 h, 96 h and

120 h for 6 global models are 58.1–69.6 km, 101.5–117.3 km, 154.2–210.6 km, 217.3–339.9 km and 316.4–503.6 km, respectively, while those in the regional models are 73.9–79.9 km, 121.2–164.5 km, 216.2–243.2 km, 370.3–352.2 km and 506.0–533.3 km, respectively (Fig. 2.6).

## **(2) Assessment of TC Intensity Forecasts**

In 2018, the absolute mean error ranges of the 5 official subjective intensity forecasts for 24 h, 48 h, 72 h, 96 h and 120 h are 4.2–5.2 m/s, 5.3–6.5 m/s, 5.8–7.1 m/s, 6.9–8.5 m/s and 7.1–10.9 m/s, respectively. The overall performance of subjective intensity prediction is better than that in 2017.

The overall performance of TC intensity prediction by the statistical prediction method in the objective forecasts is still slightly better than that of the numerical model, but the gap between the numerical prediction and the statistical prediction is gradually narrowing.

**Contact Information:** Shanghai Typhoon Institute

## **2.5 Advances in TC Real-Time Observations**

### **(1) FY-4A Temporally Intensive Regional Observations for TCs over the Northwestern Pacific and the South China Sea**

The Level 1 (L1) data of the atmospheric infrared hyper-spectral vertical detector aboard on FY-4A geostationary meteorological satellite has been officially available to international users since January 24, 2019, providing a stable monitoring service for all the typhoons in the northwestern Pacific and the South China Sea in 2019. During typhoon Lekima (1909), based on the observation sensitive area obtained by the GRAPES singular vector, the prediction target area was selected, and the demand of regional rapid observation by the GIIRS was raised. After 30 minutes of temporally intensive observations, the data were assimilated into the GRAPES model. Finally the northward moving path prediction and 24–72 h intensity prediction of Lekima were improved to a certain extent (Fig. 2.7). Since 0600 UTC on August 13, L1 data has been further upgraded from V1 to V2, improving the calibration accuracy and the data producing speed.

### **(2) Upgrading and Application of Meteorological Observation Product System**

The Meteorological Observation Center of CMA comprehensively upgraded the integrated meteorological observation product system (Tianyan) in 2019 through the new researches of multiple data quality

control and observation product algorithms. The system covers eight types of meteorological observation data, including weather radar, wind profile radar, lightning, ground observation, upper-air observation, water vapor, soil moisture and atmospheric compositions. The system also can synchronously display the monitoring and early warning information and multi-radar data flow products in customized areas. The product quality is reliable and the displaying forms are diverse. The typhoon observation products obtained by Tianyan system , such as weather radar mosaic, combined wind field and typhoon vertical products, have been successively applied in the typhoon forecasting and services, such as in Danas, Lekima, Bailu and Lingling, and the effect is notable (Fig. 2.8).

### **(3) Field Experiment Observation of Lekima**

Lekima is a super typhoon landing on Zhejiang on August 10, 2019. It maintained for a long time after the landfall, and caused heavy disasters to East China. According to the observation plan made before the test, Shanghai Typhoon Institute carried out field experiment observations before and after the landfall of Lekima. On August 8 of 2019, the Shanghai Typhoon Institute observation team set out to Zhoushan, the right front of the Lekima's moving direction, and then carried out the special observation on August 9, 2019. A variety of unconventional and temporally intensive observation data, such as wind profile, raindrop spectrum, laser wind radar, automatic station and sounding are obtained,

establishing a dataset in the TC center and its vicinity. This dataset provides valuable information for the studies of typhoon structure variation and energy transfer between different levels of the atmosphere. In addition, the ozone detection was carried out in the typhoon circulation for the first time in China (Fig. 2.9).

**Contact Information:** National Satellite Meteorological Center  
Meteorological Observation Center  
Shanghai Typhoon Institute

## **2.6 Advances in Scientific Researches on Tropical Cyclones**

(1) **The contribution of surface re-evaporation to the precipitation of landing typhoon has been studied.** By using the high resolution numerical model and ensemble prediction method, it is found that the water vapor content in the typhoon core decreases due to the influence of the surface re-evaporation process on the surface heat flux and the inflow of the boundary layer, leading to the decrease of the precipitation brought by the landing typhoon. Its contribution to the precipitation of typhoon core can reach 15%–20% (Fig. 2.10).

(2) **The evolution of the TC warm core and its related mechanism during the concentric eyewall formation.** It is found that the formation of TC concentric eyewall is a process of axisymmetrization in the boundary layer, after the outer spiral rain belt is triggered in the

upper levels and transferred to the boundary layer. During the formation of the concentric eye wall, the warm ring is generated mainly due to the sinking and warming in the edge of the inner eyewall.

**(3) Analysis of the precipitation asymmetry during the landfall of TCs in Guangdong.** It is found that the vertical shear is the main factor for the asymmetric precipitation of TCs. There is no significant change in the phase or amplitude of the asymmetric precipitation 24 h before and 12 h after the landfall (Fig. 2.11).

**(4) Analysis of the turbulent characteristics in the TC boundary layer based on the aircraft observation.** By using the boundary layer data of 6 typhoon cases observed by Hong Kong aircrafts, it is found that the momentum flux and turbulent kinetic energy increase with the wind speed, although the increase rate is very low at the high wind speed. Before the wind speed reaches 40 m/s, the vertical turbulent diffusion coefficient  $K$  is close to the logarithmic increase with the wind speed, and the mixing length is close to the constant number of 100 m. This study can be used as a reference to evaluate and improve the turbulence parameterization of TC models. It is indicated that the large-turbulent mixing near the top of the inflow layer in the eyewall region cannot be ignored in the numerical models (Fig. 2.12).

**(5) Under the influence of environmental wind shear, the typhoon rain belt has the characteristics of mesoscale convective**

**complex.** The dynamic and thermal effect of stratus area can produce continuous radial inflow in the middle troposphere, and then it goes down to the boundary layer, enhancing the tangential wind in the boundary layer on the leeward side of the stratus and increasing the scale of the typhoon vortex. In this way, it improves the inertial stability of the atmosphere and the efficiency of convection generation. Therefore, convection cells are constantly triggered in the secondary rain belt, and then develop and gather in the inner side of the s stratus, forming a linear convection system. Thus, the inflow in the boundary layer is further enhanced, so is the tangential wind. Accompanying with the axisymmetrization, this positive feedback process (tangential wind—atmospheric inertial stability— convection—radial inflow) promotes the formation of the outer eyewall (Fig. 2.13).

(6) **Differences of the rainfall microphysical characteristics.** In different rainfall areas of TCs, the microphysical characteristics of rainfall are different due to different generation mechanisms. Based on the surface raindrop spectrum data collected when typhoon Fitow passed through Shanghai World Expo station on October 6–7, 2013, the characteristics and evolution of raindrop size distribution (RSD) in the outer rain belt of Fitow and sea land front rain belt (generated by the typhoon and northerly weak cold air when the typhoon circulation gradually disappeared) are compared and analyzed. The results show that

the outer rainband and the coastal-front rain have different rainfall parameters, three Gamma Model parameters, radar reflectivity-rain rate (Z-R) and shape-slope ( $\mu-\Lambda$ ) relationship. The concentration of outer rainband at all-level raindrop diameter is higher than that of coastal-front rain, and its raindrop spectrum is wider, resulting in a higher rainfall rate of outer rainband. Since outer rainband and coastal-front rain have different Z-R relationships, it is recommended to use variable Z-R relationship for quantitative precipitation estimation in different rainfall areas of TC. In addition, as the rainfall in the outer rain belt of Fitow and the rain belt of the sea land front has different characteristics of raindrop spectrum evolution (the growth process of rainfall particles) with the increase of rainfall rate, it also implies that different microphysical parameterization schemes may be needed in different typhoon belts in the future (Fig. 2.14).

**Contact Information:** Chinese Academy of Meteorological Sciences

Guangzhou Institute of Tropical and Marine Meteorology

Shanghai Typhoon Institute

## **2.7 Improving Typhoon Forecasting and Warning Services, and Disaster Emergency Rescue**

**(1) In response to meteorological disasters such as typhoon, China has initially established a prevention mechanism and an emergency response system for meteorological disasters, led by the**

**Party committee and the government and also widely participated by social forces.** Departments of meteorology, emergency management, water resources, natural resources, ecological environment, culture and tourism, transportation and other departments have established some working mechanisms, such as joint early warning, joint information release, joint research, joint issuance of documents, joint consultation on major meteorological disasters, and a co-management mechanism between departments led by the meteorological forecasts. It timely serves the government, departments of emergency management, water conservancy, education, agriculture, fishery, maritime and other departments, providing accurate information of weather forecasts and early warnings. The Ministry of Emergency Management of the PRC (MEM) dispatches to take concrete measures ahead of disasters, to produce good predictions for disaster and risk prevention.

**(2) The MEM scientifically studies and judges the evolution of disaster, timely starts emergency response, guides local emergency rescue work, and practically provides necessities for the affected people.** Before and after the TC landfall, the MEM enters the emergency state in an all-round way. The meteorological department intensifies the discussion with the departments of water conservancy, natural resources and others on the disaster situation, analyzing the trend of the rain, water and flood. The MEM starts the emergency response according to the

development of the situation, and guides the affected people to start the emergency relief work. At the same time, according to the disaster situation, the MEM actively consults with the Ministry of Finance to calculate and arrange the disaster relief fund from the central government, supporting the governments in the disaster-stricken area for the disaster relief.

**(3) Enhancing the publicity, releasing typhoon forecast and early warning information through multiple channels, and providing good conditions for the disaster relief.** An early warning information release system is established. It covers the four executive levels, including the country, the province, the city and the county. With the help of new media and new technology, an information dissemination channel for early warnings is built with a wide coverage and the media integration. We actively optimizes the public meteorological services by providing forecasts and early warning information through [www.weather.com.cn](http://www.weather.com.cn), China Weather TV, Weather Master APP, CMA official Weibo and WeChat, as well as television, radio, website, SMS, electronic display, voice telephone, rural loud speakers, warning towers, bus-/subway-borne TV and village-based access and communication projects. Through *Xinhua News Agency*, *People's Daily*, *CCTV* and new media communication channels such as *Tik tok*, the information of disasters and related relief is released in real time to promote both publicity and

emergency response. The time interval of warning release has been shortened from 10 minutes to 5–8 minutes, with the coverage of public messages reaching 86.4%, which has brought about significant benefits in typhoon disaster prevention and mitigation.

**Contact Information:** Disaster Reduction Centre, Ministry of Emergency Management of the People’s Republic of China

Department of Emergency Response, Disaster Mitigation and Public Services, CMA

## **2.8 CMA TC Operational Training Activities**

### **(1) The Typhoon Committee Roving Seminar 2019**

According to the annual work plan of the Typhoon Committee Training and Research Coordination Group (TRCG), the 2019 Roving Seminar of TRCG is hosted by China. The theme of the Roving Seminar is typhoon quantitative precipitation estimation (QPE) and quantitative precipitation forecast (QPF). This seminar will be officially opened in the headquarters of CMA on November 11, 2019.

### **(2) The 4th CMA Typhoon Forecaster Training Programme**

As a part of Typhoon Committee TRCG’s training activities, CMA plans to host the 4<sup>th</sup> CMA International Training Programme on Typhoon Monitoring and Forecasting on 11~21 November 2019. 4 forecasters from Typhoon Committee members and 4 from Panel on Tropical Cyclones members will attend the training programme in 2019. The

training courses focus on the development and application of Dvorak technology, typhoon genesis, track and intensity forecasts, typhoon structure and its variation, typhoon storm surge, etc.

### **(3) The 66th Pre-Post Training for Weather Forecasters**

From March to June in 2019, the 66th Pre-Post Training for Weather Forecasters was held in the CMA Training Centre. 30 participants attended the course. The TC training courses covered tropical weather analysis, typhoon monitoring and forecasting, including 8 classes of teaching and 4 classes of practice.

### **(4) International Training Courses on CMA FY Satellites' Application**

WMO Nanjing Regional Training Centre held international training courses on CMA FY satellites' application during May 28-June 17, 2019. This training mainly focused on FY meteorological satellite products and remote sensing technology for countries along the Belt and Road. 29 international participants attended trainings.

### **(5) The International Workshop on the Application of Meteorological Satellite Products for Countries along the Belt and the Road**

In June of 2019, The International Workshop on the Application of Meteorological Satellite Products for Countries along the Belt and the Road was successfully held at the CMA Training Centre. This workshop

focused on improving meteorological services of FY satellites in the countries along the Belt and Road. 12 international trainees were recruited from 12 countries along the Belt and Road, including Russia, Thailand, Philippines, Iraq, Malaysia, Tajikistan, Mozambique, Egypt, Swaziland, Kenya, Sudan and Papua New Guinea. The courses mainly covered the application of FY satellite products (including the application of satellite data in TCs), operational platform SWAP and WMO satellite plan.

#### **(6) The 20th Training Workshop on the Application of Satellite Products in Weather Analyses and Forecasts**

In June of 2019, the 20th Training Workshop on the Application of Satellite Products in Weather Analyses and Forecasts was held at the CMA Training Centre. 40 trainees participated in the workshop. The training mainly included the development of FY-4 satellite, principles of its application and the application of FY-4 satellite products in different fields such as weather analyses and numerical forecasts. Four classes focused on the application of FY-4 satellite products in the monitoring of typhoon rainstorms, including the application of domestic and foreign meteorological satellites in the typhoon monitoring and the prospect of the application of FY-4 geostationary meteorological satellite products.

#### **(7) Courseware Resources Newly Added to China Meteorological Distance Education Network**

14 classes of courseware resources related to typhoons are newly added to China Meteorological Distance Education Network. The contents of the courseware include the structure, formation and path of typhoons (Lecture 9 of *Advanced Synoptic Science*), as well as strong convection and rainstorm of typhoons. Now there are 19 classes of typhoon-related courseware. From January to September in 2019, 895 trainees learned the courseware with total learning time of 8395 h.

**Contact Information:** National Meteorological Centre of CMA  
CMA Training Centre

# Annexes

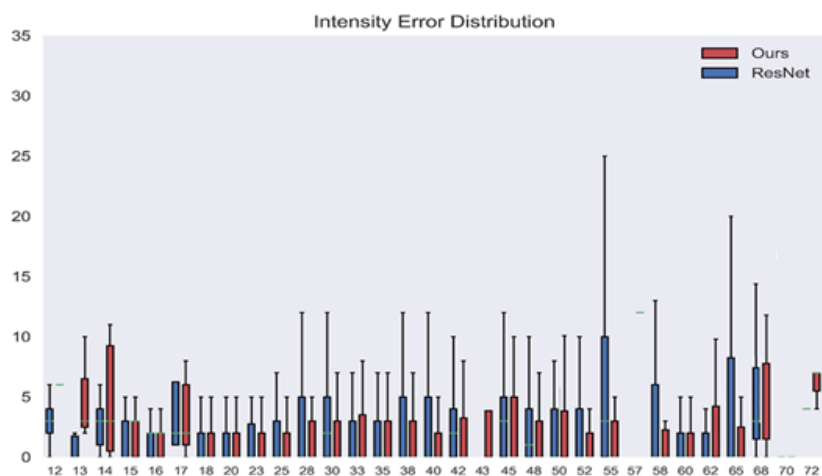


Fig. 2.1 Errors of typhoon intensity between the simulations by artificial intelligence and the observations



Fig. 2.2 Image of WIS home page

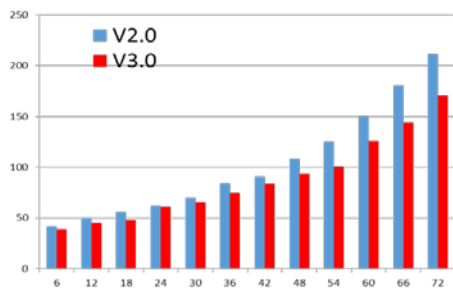


Fig. 2.3a TC track forecast errors in 2017

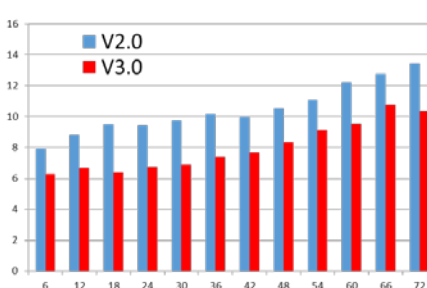


Fig. 2.3b TC intensity forecast errors in 2017

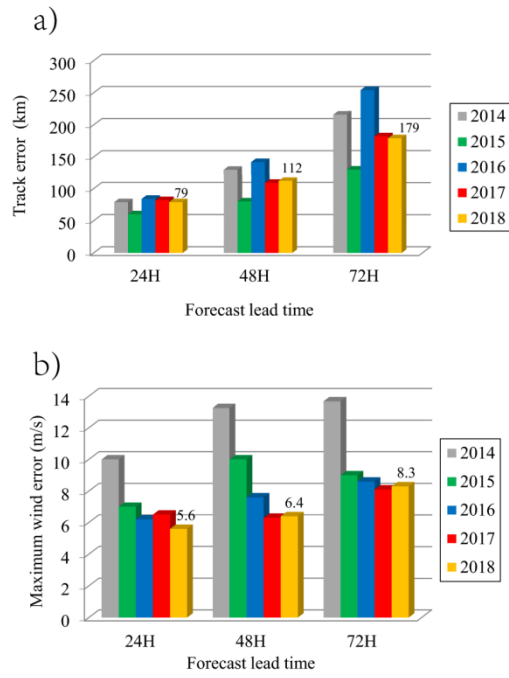


Fig. 2.4 Verification of T-RAPS's typhoon track and intensity forecast errors during 2014 – 2018

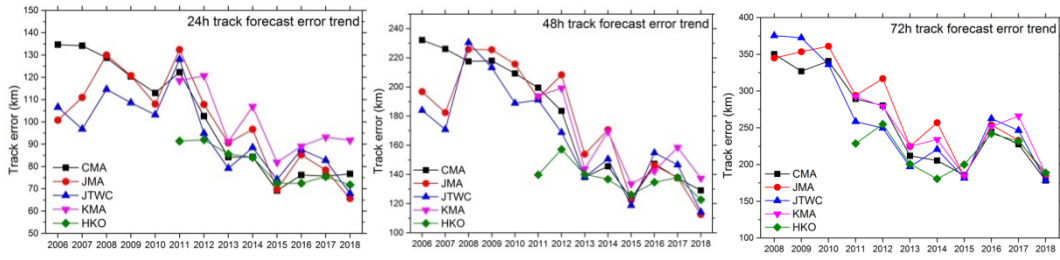


Fig. 2.5 Typhoon official track forecast errors

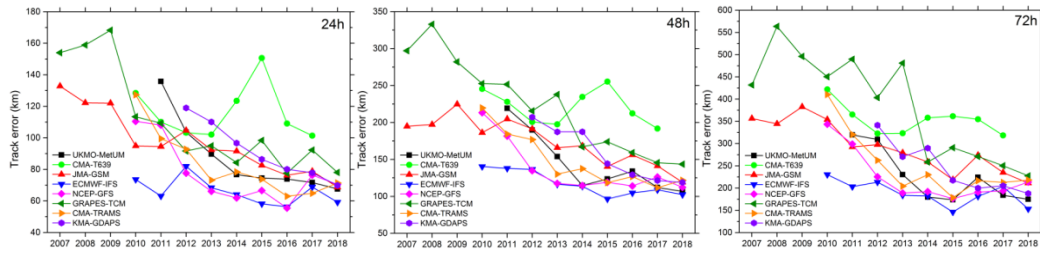


Fig. 2.6 Typhoon track forecast errors by global and regional models

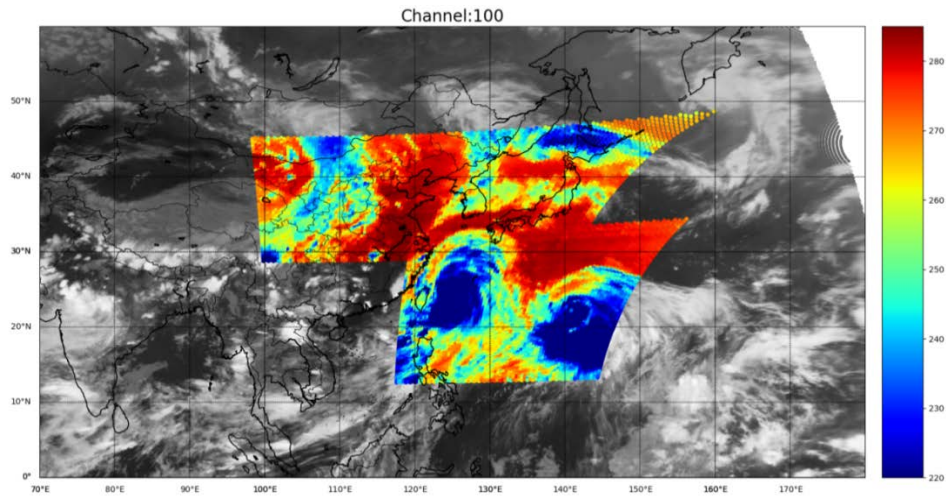


Fig. 2.7 Target observation of Lekima by satellite

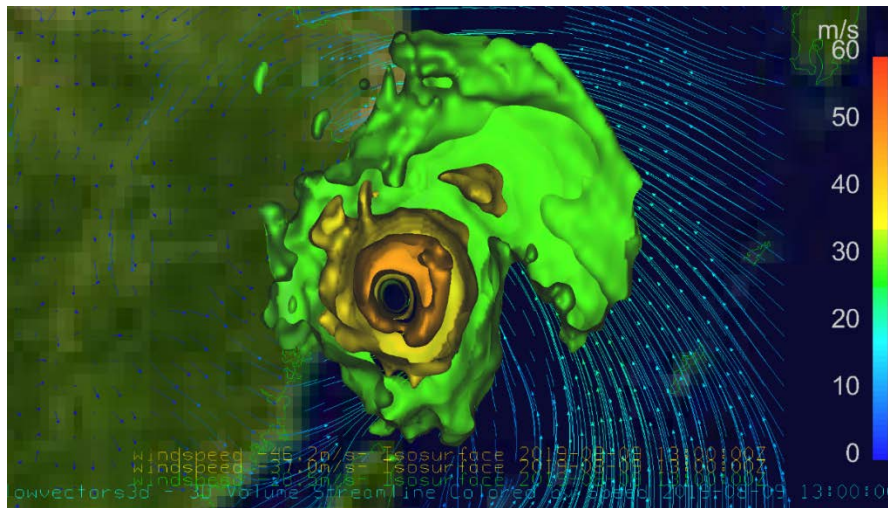


Fig. 2.8 Lekima's wind structure for level of 975 - 1000 hPa at 2100 UTC on August 9



Fig. 2.9 Launch of sounding balloon in Zhoushan on August 9, 2019

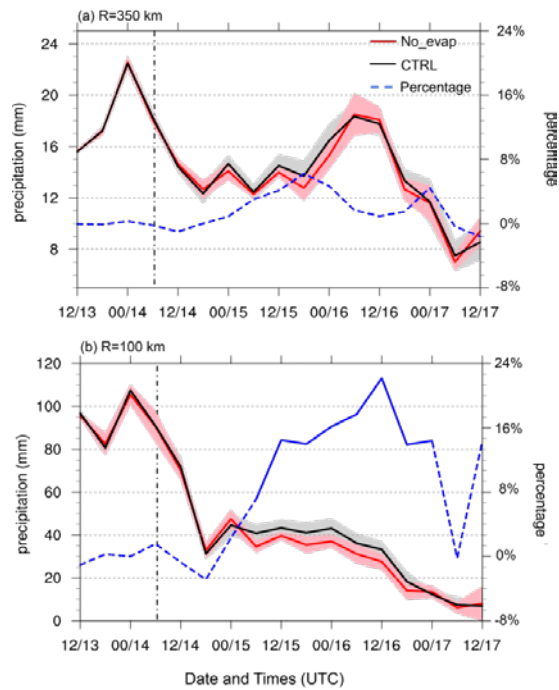


Fig. 2.10 Variation of regional averaged 6-h accumulated rainfall with time, including: (a) precipitation within the 350-km radius and (b) precipitation within the 100-km radius (control experiment, black line; sensitivity experiment, red line; difference ratio: blue line)

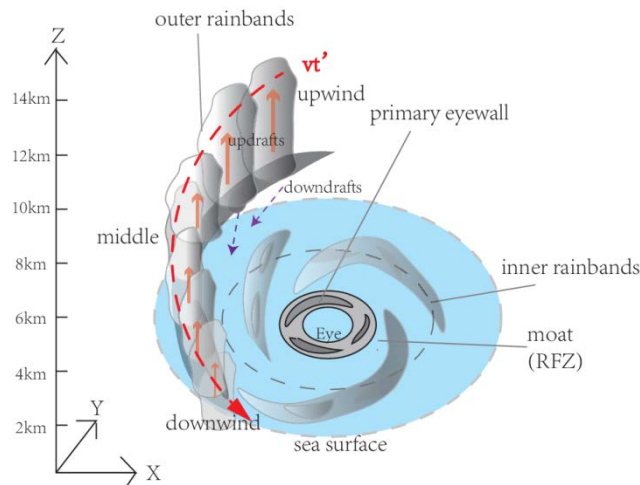


Fig. 2.11 Observation and analysis of precipitation asymmetry during TC landfall in Guangdong: (a) 24 h before landfall; (b) 12 h before landfall; (c) landfall time; (d) 12 h after landfall; and (e) precipitation asymmetry within different radii from 24 h before landfall to 12 h after landfall

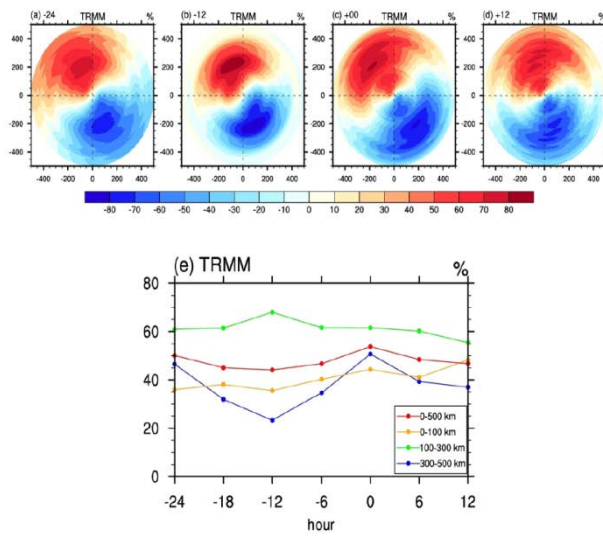


Fig. 2.12 Linear plot of vertical-vortex diffusion coefficient as a function of the average wind speed and the vertical mixing length

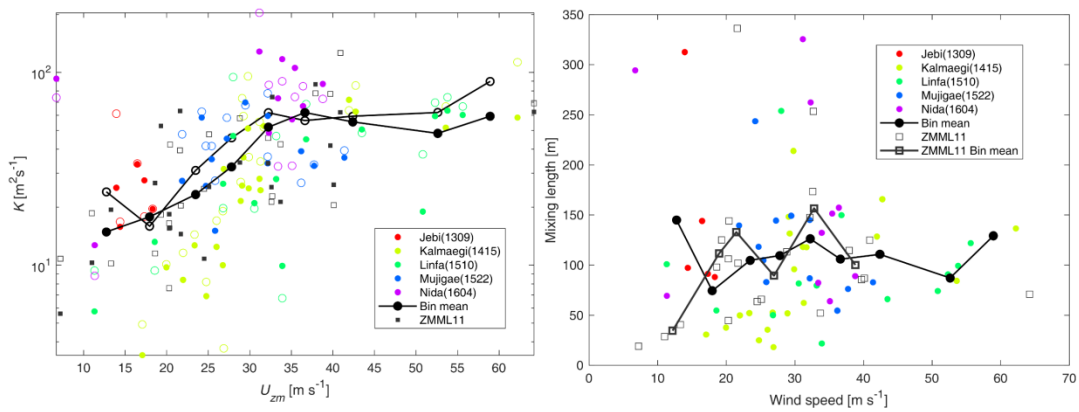


Fig. 2.13 Conceptual model of the outer eyewall formation. Yellow represents the convection system in the spiral rain belt; and purple represents the stratus; the red arrow indicates the radial flow; and the vertical wind shear is calculated according to 200 – 850 hPa high and low level wind field (direction: left to right), within 200 – 500 km radius of typhoon center

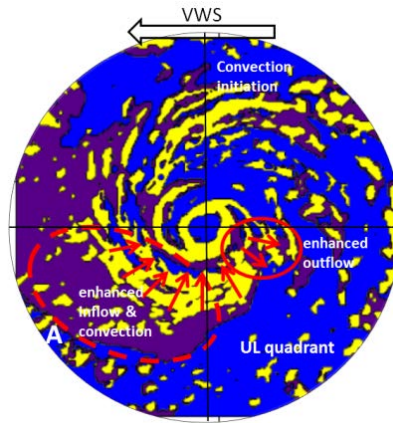


Fig. 2.14 (a) Comprehensive raindrop spectrum distribution of total rainfall (dotted line) and convective rainfall (solid line) in outer rain belt and sea land front; (b) raindrop spectrum distribution of convective rainfall in outer rain belt (solid line) and sea land front (dotted line) with different rainfall rates; (c) average concentration of particles and (d) average diameter in outer rain belt (red color) and sea land front (blue) with different rainfall rates; and (e) the ratio distribution of convective rainfall in outer rain belt (solid line) and sea land front (dotted line) with different precipitation rates to their respective comprehensive RSD

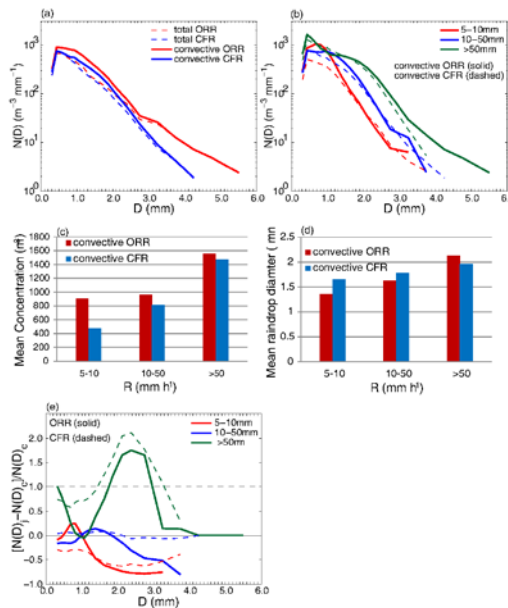


Figure 2.15 (a) Composite RSDs of total ORR (red dashed line), total CFR (blue dashed), convective ORR (red solid line) and convective CFR (blue solid line); (b) the RSDs of convective ORR (solid lines) and convective CFR (dashed lines) classified by the modified classification method at different rain rates; (c) mean concentrations and (d) mean raindrop diameters at different rain rates of convective ORR (red bars) and convective CFR (blue bars); (e) the ratio of deviation between RSD at the  $j$ th rain rate and composite RSD with respect to composite RSD for convective ORR (solid lines) and convective CFR (dashed lines)